nature chemistry

ARTICLES

PUBLISHED ONLINE: 20 JANUARY 2013 | DOI: 10.1038/NCHEM.1548

Quantitative visualization of DNA G-quadruplex structures in human cells

Giulia Biffi[1], David Tannahill[1], John McCafferty[2] and Shankar Balasubramanian[1,3]*

Four-stranded G-quadruplex nucleic acid structures are of great interest as their high thermodynamic stability under near-physiological conditions suggests that they could form in cells. Here we report the generation and application of an engineered, structure-specific antibody employed to quantitatively visualize DNA G-quadruplex structures in human cells. We show explicitly that G-quadruplex formation in DNA is modulated during cell-cycle progression and that endogenous G-quadruplex DNA structures can be stabilized by a small-molecule ligand. Together these findings provide substantive evidence for the formation of G-quadruplex structures in the genome of mammalian cells and corroborate the application of stabilizing ligands in a cellular context to target G-quadruplexes and intervene with their function.

Extensive structural and biophysical evidence confirms that certain G-rich DNA (and RNA) sequences can fold into non-canonical secondary structures, called G-quadruplexes. G-quadruplex structures comprise two or more G-tetrads that form when four guanines are held in a planar arrangement through Hoogsteen hydrogen bonding, with additional stabilization provided by a monovalent cation coordinated to the O6 lone pairs of each guanine[1]. The high thermodynamic stability of G-quadruplexes under near-physiological conditions suggests that these structures may form in genomic DNA *in vivo*, although this is a topic of some debate[2]. DNA G-quadruplex structures are associated with a number of important aspects of genome function, which include transcription, recombination and replication[3–6]. Computational analysis revealed the prevalence of G-quadruplex motifs in key regulatory regions of the human genome, such as promoters, gene bodies and untranslated regions[7–10]. G-quadruplex motifs are also present at the ends of chromosomes (telomeres), and therefore G-quadruplex structures may also be involved in maintaining chromosome stability. Indeed, telomeric DNA G-quadruplexes have been isolated from genomic DNA using small-molecule ligands[11] and, moreover, the application of such small molecules leads to cell death through the displacement of protective telomeric protein components[12,13].

Accurate replication of DNA G-quadruplex motifs requires their unfolding by helicases, including BLM (Bloom syndrome protein), FANCJ (Fanconi anaemia group J protein), REV1 and WRN (Werner's syndrome protein)[14–17], and genome-wide studies show that the predicted G-quadruplex motifs are binding sites for the helicases ATRX (alpha-thalassaemia/mental retardation

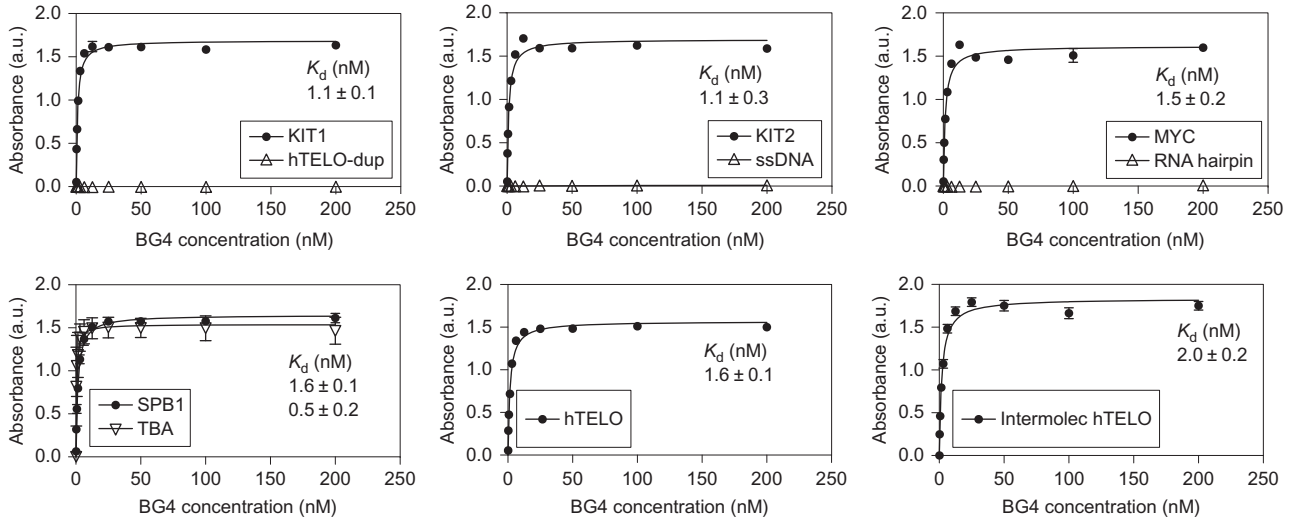

Figure 1 | Structure specificity of the BG4 antibody for G-quadruplex structures. Binding curves as determined by ELISA show that the BG4 antibody has a high affinity for intramolecular and intermolecular DNA G-quadruplex structures with negligible binding to a RNA hairpin, to double-stranded DNA (hTELO-dup) and to single-stranded DNA (ssDNA). BG4 does not show a preference for any particular G-quadruplex conformation as it binds with similar affinity to parallel propeller (KIT1, KIT2 and MYC), anti-parallel propeller (SPB1 and TBA), mixed parallel/anti-parallel propeller (hTELO) and intermolecular (intermolec hTELO) G-quadruplex structures. Dissociation constants (K_d) are indicated. Error bars represent the s.e.m. calculated from three replicates. a.u. = arbitrary units.

[1]Cancer Research UK, Cambridge Institute, Li Ka Shing Centre, Robinson Way, Cambridge, CB2 0RE, UK, [2]Department of Biochemistry, University of Cambridge, Tennis Court Road, Cambridge CB2 1QW, UK, [3]Department of Chemistry, University of Cambridge, Lensfield Road, Cambridge CB2 1EW, UK.
*e-mail: sb10031@cam.ac.uk

© 2013 Macmillan Publishers Limited. All rights reserved.

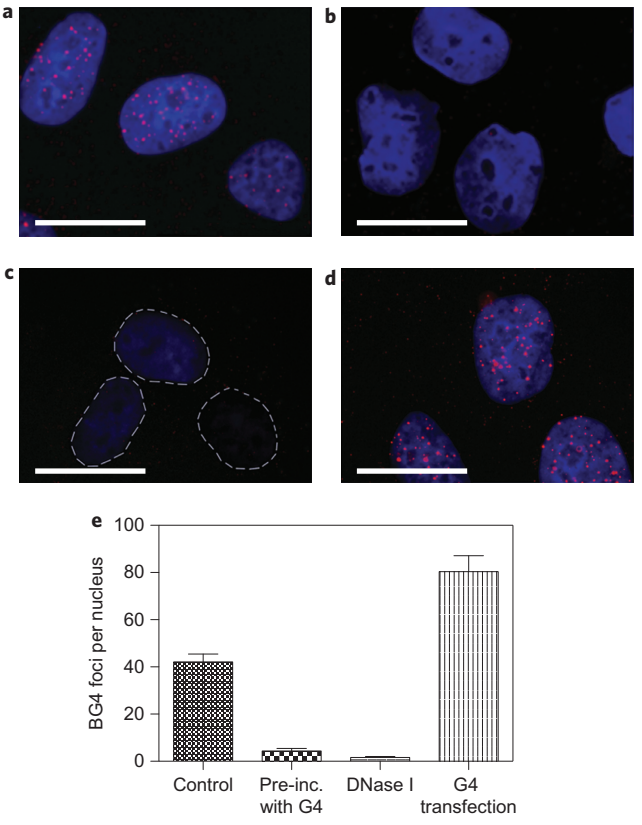

Figure 2 | Visualization of DNA G-quadruplex structures in nuclei of human cancer cells. a, Immunofluorescence showing BG4 foci (red) in U2OS osteosarcoma cell nuclei. **b**, Loss of BG4 foci in U2OS cells after pre-incubation of the antibody with pre-folded G-quadruplex oligonucleotides. **c**, Loss of BG4 foci in U2OS cells after DNase I treatment. The dotted lines show the boundary of the nuclei. **d**, Increase in BG4 foci number after transfection with pre-folded G-quadruplex oligonucleotides. The nuclei are counterstained with DAPI (blue). **e**, The quantification of BG4 foci number per nucleus for **a**–**d**. 100–200 nuclei were counted per condition and the s.e.m. was calculated from a set of three replicates. These observations support the targeting and visualization of DNA G-quadruplex structures in human cells by the BG4 antibody. Scale bars, 20 μm.

syndrome X-linked) and PIF1[18,19]. Also, our recent genome-wide study shows that a stabilizing small molecule, pyridostatin (PDS), induces DNA damage at sites enriched in G-quadruplex motifs and that PIF1 probably resolves these structures *in vivo*[5]. An important breakthrough in the field was the visualization of G-quadruplex structures at the telomeres of ciliate macronuclei in which the millions of telomeres enabled fluorescent imaging with an antibody, and revealed the cell-cycle dependent formation of telomeric G-quadruplexes[20–22]. Up to now, it has remained an important challenge to visualize G-quadruplex structures in the DNA of mammalian cells.

Herein we describe an engineered, structure-specific antibody probe that binds with high selectivity and low nanomolar affinity to DNA G-quadruplex structures. This antibody was then employed to visualize DNA G-quadruplex structures in the genomic DNA of human cells. Also, we characterize the relationship between the cell cycle and G-quadruplex formation, and also demonstrate that a small molecule G-quadruplex ligand stabilizes these structures in cells.

Results and discussion

To generate an antibody specific for G-quadruplex structures, we employed phage display with a library of 2.3×10^{10} different single-chain antibody clones[23]. Through *in vitro* selection for G-quadruplex structures, the best hit among the selected binders, called BG4, was isolated for further studies. Using enzyme-linked immunosorbent assay (ELISA) methods, we showed that BG4 has a high affinity for intramolecular and intermolecular DNA G-quadruplexes ($K_d = 0.5$–1.6 nM and 2.0 nM, respectively) with no detectable binding to a RNA hairpin, single-stranded DNA or double-stranded DNA (Fig. 1). To evaluate the affinity of BG4 for different structural conformations, we investigated the binding to parallel propeller (MYC, KIT1 and KIT2), anti-parallel propeller (SPB1 and TBA), mixed parallel/anti-parallel propeller (hTELO) and intermolecular (intermolec hTELO) G-quadruplex structures (Supplementary Fig. S1). Given the similarities in binding affinities, these results indicate that BG4 is a G-quadruplex structure-specific antibody that does not have a preference for any particular G-quadruplex conformation. Next, we characterized BG4 specificity for G-quadruplexes over other nucleic acid structures in competition experiments. Up to a 50-fold excess of different competitors was pre-incubated with the BG4 antibody before assessment of the binding to the MYC G-quadruplex by ELISA. In no case did we observe significant inhibition of binding to the target G-quadruplex by yeast tRNA, double-stranded poly $(GC)_n$ or poly $(AT)_n$, sonicated double-stranded salmon sperm

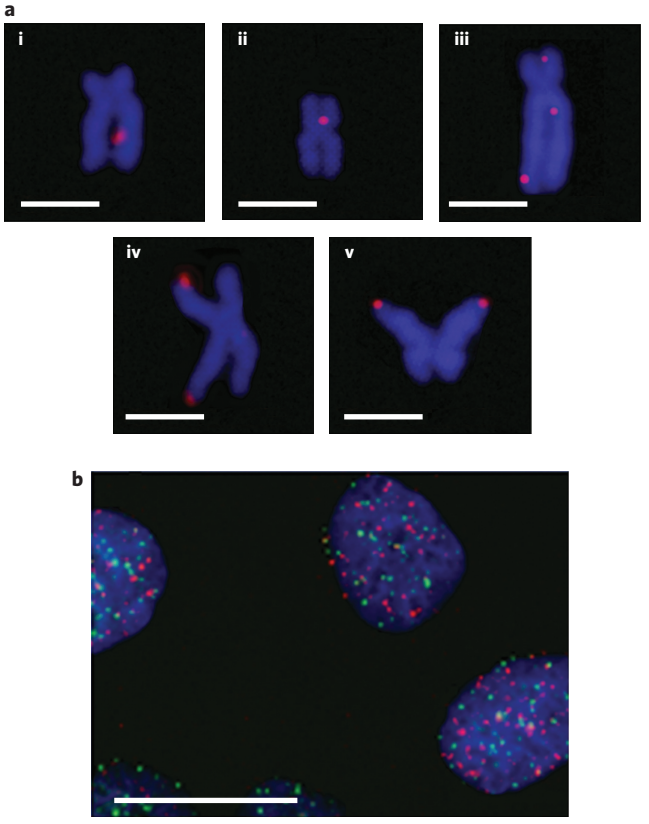

Figure 3 | Localization of G-quadruplex structures in chromosomes. **a**, Immunofluorescence for BG4 on metaphase chromosomes isolated from Hela cervical cancer cells. Discrete BG4 foci (red) were observed both within the non-telomeric regions **i**–**iii** and at the telomeres **iv** and **v**, a well-characterized site of G-quadruplex formation. The symmetrical appearance of the foci in some sister chromatids **v** supports G-quadruplex formation within the same genomic locations in newly replicated DNA. Chromosomes are counterstained with DAPI (blue). Scale bars, 2.5 μm. **b**, Absence of large co-localization between telomeric TRF2 proteins (green) and G-quadruplexes (red) in U2OS cells. This suggests that endogenous G-quadruplex structures are present largely outside the telomeres. Nuclei are counterstained with DAPI (blue). Scale bar, 20 μm.

© 2013 Macmillan Publishers Limited. All rights reserved.

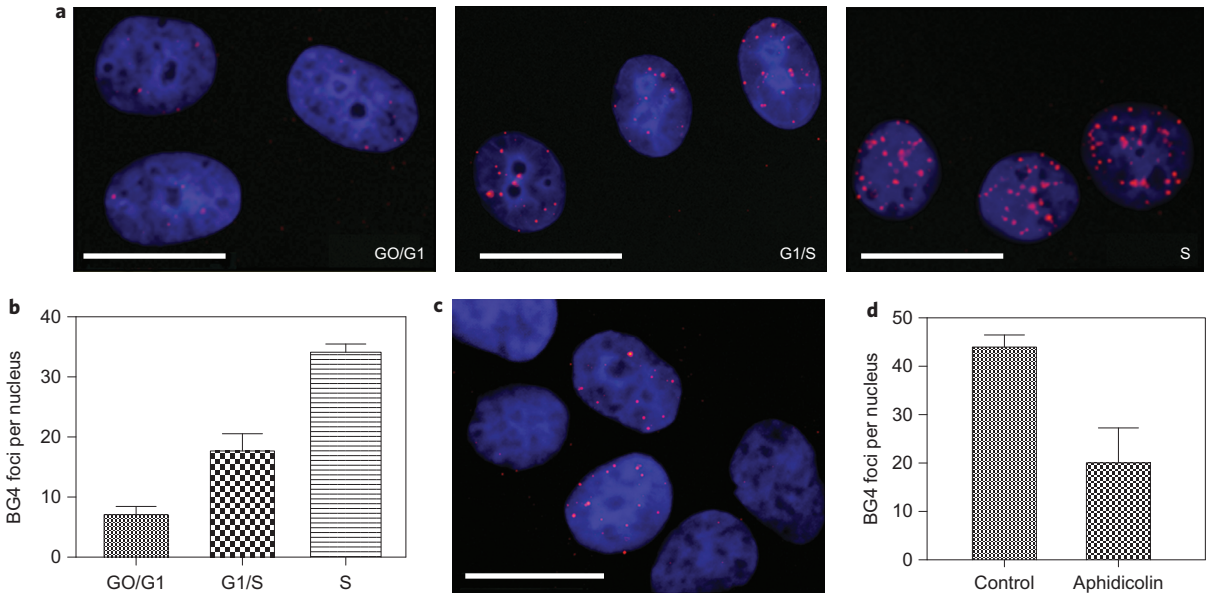

Figure 4 | Modulation of G-quadruplex structures during cell-cycle progression. a, BG4 staining in synchronized MCF-7 mammary adenocarcinoma cell populations at the G0/G1 and G1/S boundaries, and during the S phase. Nuclei are counterstained with DAPI (blue). Scale bars, 20 μm. **b**, Quantification of BG4 foci number per nucleus for **a**. 100 nuclei were counted per stage and the s.e.m. was calculated from a set of three replicates. **c**, A greater than two fold reduction in the BG4 foci number after inhibition of DNA synthesis by aphidicolin treatment (5 μM for two hours). **d**, Quantification of the BG4 foci number with or without aphidicolin treatment. 100 nuclei were counted and the s.e.m. was calculated from a set of three replicates. These experiments demonstrate that G-quadruplex structures are modulated during the cell cycle and, in particular, support the replication-dependent formation of endogenous DNA G-quadruplexes.

DNA or a RNA hairpin oligonucleotide. Competition was achieved only when a positive control KIT1 G-quadruplex oligonucleotide was used (Supplementary Fig. S2). Collectively, these experiments robustly support the specificity of the BG4 antibody for G-quadruplex structures.

Next BG4 was used to visualize DNA G-quadruplex structures in human cells. After incubation of fixed cells with BG4, sensitive detection was achieved through an amplified fluorescence signal generated by incubation with a secondary antibody and then a tertiary fluorochrome-labelled antibody. All the cell lines examined showed punctate nuclear staining (Fig. 2a and Supplementary Fig. S3), which was not observed in the absence of a primary BG4 antibody (Supplementary Fig. S3). The specificity of BG4 for G-quadruplexes was confirmed by the loss of signal on pre-incubation of the antibody with excess pre-folded G-quadruplex oligonucleotides, but no signal loss on pre-incubation with single-stranded oligonucleotides (Fig. 2b and Supplementary Fig. S3). The G-quadruplex foci also disappeared after DNase treatment (Fig. 2c), but not after RNase treatment (Supplementary Fig. S3). Moreover, the number of BG4 foci increased when cells were transfected first with pre-folded G-quadruplex oligonucleotides, but not when cells were transfected with single-stranded oligonucleotides (Fig. 2d and Supplementary Fig. S3). Taken together, these observations support the targeting and visualization of DNA G-quadruplex structures in human cells by BG4.

To corroborate further the detection of G-quadruplex structures in the cellular genome, we assessed their distribution at the level of individual chromosomes (Fig. 3a and Supplementary Fig. S4). To do this, we incubated BG4 with chromosomes prepared from cells treated with colcemid to block mitosis at metaphase, a stage of the cell cycle at which individual chromosomes are visualized most easily. That BG4 localization was found at the chromosomal ends (iv and v in Fig. 3a) confirms the presence of G-quadruplex structures at human telomeres. Furthermore, discrete BG4 foci were observed dispersed across the chromosomes (i–iii in Fig. 3a), which demonstrates that G-quadruplex structures also form outside the telomeric regions. Interestingly, in some cases we observed symmetrical staining of sister chromatids (v in Fig. 3a), which supports G-quadruplex formation within the same genomic locations in newly replicated DNA. When the number of BG4 foci was quantified in 100 individual well-spread metaphase chromosomes, the majority (58%) of chromosomes had at least one site of BG4 staining and around one-third displayed multiple foci (Supplementary Fig. S4). When we scored positive BG4 staining chromosomes for telomeric distribution, we found that the majority (~75%) of BG4 foci were present outside the telomeres (Supplementary Fig. S4). Nonetheless, the observation that ~25% of the foci were located at the telomeres is evidence of site-specific localization of the BG4 antibody to a well-characterized site of G-quadruplex formation.

When fixed cells were co-stained for BG4 and TRF2 (telomere repeat-binding factor 2), a protein localized to telomeres, the majority of BG4 foci (82.4%) did not coincide with TRF2 foci (Fig. 3b). This further suggests that endogenous G-quadruplex structures are present largely outside the telomeres. Not all the TRF2 foci co-localize with BG4 staining (36.8%) and not all metaphase chromosomes show telomeric BG4 staining. Although these observations might indicate a differential propensity of disparate telomeres to form G-quadruplex structures, they may also be accounted for by differences in antibody accessibility to the target (for example, masking by telomere-binding proteins, such as components of the protective shelterin complex).

We anticipated that G-quadruplex formation most probably occurs during DNA replication, because the associated mechanisms necessitate that duplex strands become separated at replication forks, where single-stranded DNA may fold more easily into secondary structures[15]. To investigate this, we followed the formation of G-quadruplex structures during cell-cycle progression. BG4 staining on synchronized cell populations showed the lowest levels of G-quadruplex formation at G0/G1, a phase during which no replication occurs and cellular processes are quiescent. At the G1/S checkpoint, a time when cells prepare for entry into S phase,

© 2013 Macmillan Publishers Limited. All rights reserved.

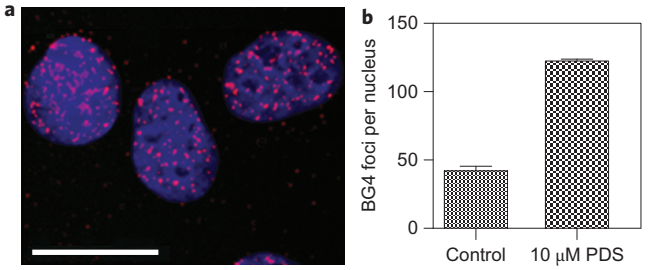

Figure 5 | Stabilization of endogenous G-quadruplex structures by a small-molecule ligand. a, Increase in BG4 foci number in U2OS cells after treatment with the G-quadruplex binding ligand PDS. Nuclei are counterstained with DAPI (blue). Scale bar, 20 μm. **b**, Quantification of BG4 foci number per nucleus with or without PDS treatment. 200 nuclei were counted per condition and the s.e.m. was calculated from three replicates. After PDS treatment, a marked increase (~2.9-fold) in nuclear staining was observed. These results indicate that, at the pertinent sites, PDS traps endogenous G-quadruplex structures to increase the number of BG4 targets available.

the period when DNA replication occurs, there was a ~2.5-fold increase in the number of BG4 foci. During S phase, the number of BG4 foci was maximal (~4.8-fold more than at G0/G1), which is consistent with the replication-dependent formation of G-quadruplex structures (Fig. 4a,b). To confirm that the increase in G-quadruplex structures observed during the S phase was, indeed, dependent on DNA replication, we blocked cellular DNA synthesis with aphidicolin, a tetracyclic diterpene that specifically inhibits DNA polymerase α activity. As expected, aphidicolin treatment led to a large (over two fold) reduction in the number of BG4 foci (Fig. 4c,d). These experiments demonstrate that G-quadruplex structures are modulated during the cell cycle in a manner that is sensitive to whether or not the DNA is being replicated.

The small-molecule ligand PDS is reported to stabilize G-quadruplex structures and displace bound proteins[5,11,13,24]. Therefore, we rationalized that the application of PDS to cells would result in the detection of more DNA G-quadruplex targets by the BG4 antibody. Indeed, when cells were treated with PDS, there was a marked increase (~2.9-fold) in nuclear staining (Fig. 5a,b) that disappeared after DNase treatment (Supplementary Fig. S5). This increase is not caused by a change of the BG4 binding affinity for G-quadruplex structures in the presence of PDS, because there was no effect of PDS on BG4 binding as judged by ELISA (Supplementary Fig. S5). These results indicate that, at pertinent sites, PDS traps G-quadruplex structures to increase the number of BG4 targets available. This confirms the proposal in earlier work that small-molecule ligands interact directly with cellular DNA to stabilize G-quadruplexes that, if not resolved, lead to DNA damage[5,13].

Table 1 | Oligonucleotides used in enzyme-linked immunosorbent assays.

Name	Sequence
hTELO	5′-GG(TTAGGG)$_4$TTAG-3′
hTELO-dup	5′-GG(TTAGGG)$_4$TTAG-3′/3′-C(AATCCC)$_4$AAT-5′
ssDNA	5′-GGCATAGTGCGTGGGCG-3′
MYC	5′-TGAGGGTGGGTAGGGTGGGTAA-3′
KIT1	5′-AGGGAGGGCGCTGGGAGGAGGG-3′
KIT2	5′-CGGGCGGGCGCGAGGGAGGGG-3′
SPB1	5′-GGCGAGGAGGGGCGTGGCCGGC-3′
TBA	5′-GGTTGGTGTGGTTGG-3′
RNA hairpin	5′-CAGUACAGAUCUGUACUG-3′
intermolec hTELO	5′-(TTAGGG)$_3$-3′

In summary, we have developed a highly specific DNA G-quadruplex antibody and employed it to visualize G-quadruplex structures in the DNA of human cells. We demonstrated how the formation of G-quadruplexes is dynamically sensitive to the cell cycle, and showed by direct visualization that a small-molecule ligand traps these structures in cells. An insightful future goal is to generate, by sequencing, a map of the precise locations of G-quadruplex structures at a genome-wide level. Our new findings therefore provide an important basis to help underpin recent chemical biological and genetic studies that highlight a range of potentially important biological roles of G-quadruplex structures.

Methods

Phage-display selection. A single-chain antibody, BG4, was isolated from the Sanger phage-display library[23] (2.3×10^{10} single-chain antibody clones) through selection using a panel of intramolecular G-quadruplex structures. Two rounds of selection in solution were carried out using streptavidin-coated beads (Dynabeads M-280 Streptavidin, Invitrogen) with 1 μM of biotinylated G-quadruplex oligonucleotides for the first round of selection and 100 nM for the second round. Then the selected binders were cloned into the pSANG10 expression plasmid for antibody production. Screening of the selected binders was performed by dissociation-enhanced lanthanide fluorescent immunoassay (DELFIA) using an anti-FLAG europium-conjugated antibody (Sigma) and the DELFIA reagent (Perkin Elmer). Signal intensity was detected at 615 nm with a PHERAstar microplate reader (BMG Labtech) using time-resolved fluorescence detection.

Circular dichroism (CD) spectroscopy. For CD spectroscopy, 5 μM DNA G-quadruplex oligonucleotides were annealed in 10 mM Tris HCl, pH 7.4, 100 mM KCl by slow cooling from 95 °C to 21 °C. Five scans were performed from 200 to 320 nm using a Jasco J-810 spectropolarimeter with the buffer spectrum subtracted and zero correction at 320 nm.

Enzyme-linked immunosorbent assay. ELISAs for binding affinity and specificity were performed using standard methods. Briefly, biotinylated oligonucleotides (Table 1) (biomers.net GmbH) were bound to streptavidin-coated plates followed by incubation with BG4 (and PDS for Supplementary Fig. S5), and detection was achieved with an anti-FLAG horseradish peroxidase (HRP)-conjugated antibody (ab1238, Abcam) and TMB (3,3′,5,5′-tetramethylbenzidine, HRP substrate, Roche). Signal intensity was measured at 450 nm on a PHERAstar microplate reader (BMG Labtech). Dissociation constants were calculated from binding curves using GraphPad Prism (GraphPad Software Inc.) and standard error of mean (s.e.m.) values were calculated from three replicates. G-quadruplex oligonucleotides were annealed in 10 mM Tris HCl, pH 7.4, 100 mM KCl by slow cooling from 95 °C to 21 °C.

For competition experiments, before the assessment of BG4 binding to the MYC G-quadruplex by ELISA, BG4 was pre-incubated for one hour at room temperature (21 °C) with 0, 1, 5, 10, 20 and 50 equiv. of either KIT1 (G-quadruplex), RNA hairpin, yeast tRNA, double-stranded sonicated salmon sperm DNA, double-stranded poly(GC)$_n$ or poly(AT)$_n$.

Cell cultures and immunofluorescence. U2OS (osteosarcoma), HeLa (cervical carcinoma), HT1080 (fibrosarcoma), MCF-7 (mammary adenocarcinoma) and MDA-MB-231 (breast carcinoma) cells were cultured in Dulbecco's modified Eagle medium (DMEM) (Gibco), 1% L-glutamine and 10% fetal bovine serum (FBS); MRC-5 (fetal lung fibroblasts) cells were cultured in Eagle's minimum essential medium (Sigma) and 10% FBS; and MCF-10A (mammary epithelial) cells were cultured in mammary epithelial cell growth medium (Lonza) with cholera toxin (at 37 °C with 5% CO_2). Cells grown on glass coverslips were fixed in 2% paraformaldehyde/PBS or in methanol/acetic acid (3:1) (Supplementary Fig. S3) and permeabilized with 0.1% triton-X100/PBS. After blocking in 2% Marvel/PBS, immunofluorescence was performed using standard methods with BG4, anti-FLAG (No. 2368, Cell Signaling Technology) and anti-rabbit Alexa 594-conjugated (A11037, Invitrogen) antibodies. Coverslips were mounted with Prolong Gold/DAPI (4′,6-diamidino-2-phenylindole, Invitrogen). For TRF2 detection, anti-TRF2 (ab13579, Abcam) and anti-mouse Alexa 488-conjugated (A11029, Invitrogen) antibodies were used. For enzyme treatments, coverslips were incubated after permeabilization with 120 U of Turbo DNase (0.12 U μl^{-1}) or 50 μg ml^{-1} RNase A (Ambion) for one hour at 37 °C. For pre-incubation experiments, BG4 was incubated with a 20-fold excess of pre-folded DNA G-quadruplexes or single-stranded DNA oligonucleotides. Oligonucleotide transfections were performed using 200 nM pre-annealed DNA G-quadruplexes or single-stranded DNA oligonucleotides and TransIT-Oligo transfection reagent (Mirus). For PDS treatment, cells were incubated with 10 μM of the compound for 24 hours. For metaphase preparations, cells were treated with colcemid (50 ng ml^{-1}) for two hours before resuspension in 0.075 mM KCl for 30 minutes at 37 °C. Cells were then fixed in methanol/acetic acid (3:1) before spreading on slides. 100 well-spread metaphase chromosomes were analysed for the number and localization of BG4 foci. For cell synchronization, MCF-7 cells were

© 2013 Macmillan Publishers Limited. All rights reserved.

incubated for 24 hours in serum-free DMEM (G0/G1), grown for 16 hours in DMEM, 20% FBS and 200 μM mimosine (G1/S), and for three hours in DMEM and 10% FBS (S phase). Cell-cycle stages were confirmed using a fluorescent-activated cell sorter (FACSCalibur, BD Biosciences). To inhibit DNA replication, cells were incubated with 5 μM aphidicolin for two hours. Digital images were recorded using a DP70 camera (Olympus) on an Axioskop 2 plus microscope (Zeiss) and analysed with Volocity software (Perkin Elmer). 100–200 nuclei were counted per condition and the s.e.m. was calculated from three replicates. Frequency distribution graphs were plotted using GraphPad Prism (GraphPad Software Inc.).

Received 17 October 2012; accepted 6 December 2012; published online 20 January 2013

References

1. Sen, D. & Gilbert, W. Formation of parallel four-stranded complexes by guanine-rich motifs in DNA and its implications for meiosis. *Nature* **334,** 364–366 (1988).
2. Lipps, H. J. & Rhodes, D. G-quadruplex structures: *in vivo* evidence and function. *Trends Cell Biol.* **19,** 414–422 (2009).
3. Cahoon, L. A. & Seifert, H. S. An alternative DNA structure is necessary for pilin antigenic variation in *Neisseria gonorrhoeae*. *Science* **325,** 764–767 (2009).
4. Cheung, I., Schertzer, M., Rose, A. & Lansdorp, P. M. Disruption of dog-1 in *Caenorhabditis elegans* triggers deletions upstream of guanine-rich DNA. *Nature Genet.* **31,** 405–409 (2002).
5. Rodriguez, R. *et al.* Small-molecule-induced DNA damage identifies alternative DNA structures in human genes. *Nature Chem. Biol.* **8,** 301–310 (2012).
6. Siddiqui-Jain, A., Grand, C. L., Bearss, D. J. & Hurley, L. H. Direct evidence for a G-quadruplex in a promoter region and its targeting with a small molecule to repress c-MYC transcription. *Proc. Natl Acad. Sci. USA* **99,** 11593–11598 (2002).
7. Eddy, J. & Maizels, N. Gene function correlates with potential for G4 DNA formation in the human genome. *Nucleic Acids Res.* **34,** 3887–3896 (2006).
8. Eddy, J. & Maizels, N. Conserved elements with potential to form polymorphic G-quadruplex structures in the first intron of human genes. *Nucleic Acids Res.* **36,** 1321–1333 (2008).
9. Huppert, J. L. & Balasubramanian, S. Prevalence of quadruplexes in the human genome. *Nucleic Acids Res.* **33,** 2908–2916 (2005).
10. Todd, A. K., Johnston, M. & Neidle, S. Highly prevalent putative quadruplex sequence motifs in human DNA. *Nucleic Acids Res.* **33,** 2901–2907 (2005).
11. Muller, S., Kumari, S., Rodriguez, R. & Balasubramanian, S. Small-molecule-mediated G-quadruplex isolation from human cells. *Nature Chem.* **2,** 1095–1098 (2010).
12. Gomez, D. *et al.* Telomestatin-induced telomere uncapping is modulated by POT1 through G-overhang extension in HT1080 human tumor cells. *J. Biol. Chem.* **281,** 38721–38729 (2006).
13. Rodriguez, R. *et al.* A novel small molecule that alters shelterin integrity and triggers a DNA-damage response at telomeres. *J. Am. Chem. Soc.* **130,** 15758–15759 (2008).
14. Crabbe, L., Verdun, R. E., Haggblom, C. I. & Karlseder, J. Defective telomere lagging strand synthesis in cells lacking WRN helicase activity. *Science* **306,** 1951–1953 (2004).
15. Sarkies, P., Reams, C., Simpson, L. J. & Sale, J. E. Epigenetic instability due to defective replication of structured DNA. *Mol. Cell* **40,** 703–713 (2010).
16. Sun, H., Karow, J. K., Hickson, I. D. & Maizels, N. The Bloom's syndrome helicase unwinds G4 DNA. *J. Biol. Chem.* **273,** 27587–27592 (1998).
17. Wu, Y., Shin-ya, K. & Brosh, R. M. Jr. FANCJ helicase defective in Fanconia anemia and breast cancer unwinds G-quadruplex DNA to defend genomic stability. *Mol. Cell Biol.* **28,** 4116–4128 (2008).
18. Law, M. J. *et al.* ATR-X syndrome protein targets tandem repeats and influences allele-specific expression in a size-dependent manner. *Cell* **143,** 367–378 (2010).
19. Paeschke, K., Capra, J. A. & Zakian, V. A. DNA replication through G-quadruplex motifs is promoted by the *Saccharomyces cerevisiae* Pif1 DNA helicase. *Cell* **145,** 678–691 (2011).
20. Paeschke, K. *et al.* Telomerase recruitment by the telomere end binding protein-beta facilitates G-quadruplex DNA unfolding in ciliates. *Nature Struct. Mol. Biol.* **15,** 598–604 (2008).
21. Paeschke, K., Simonsson, T., Postberg, J., Rhodes, D. & Lipps, H. J. Telomere end-binding proteins control the formation of G-quadruplex DNA structures *in vivo*. *Nature Struct. Mol. Biol.* **12,** 847–854 (2005).
22. Schaffitzel, C. *et al. In vitro* generated antibodies specific for telomeric guanine-quadruplex DNA react with *Stylonychia lemnae* macronuclei. *Proc. Natl Acad. Sci. USA* **98,** 8572–8577 (2001).
23. Schofield, D. J. *et al.* Application of phage display to high throughput antibody generation and characterization. *Genome Biol.* **8,** R254 (2007).
24. Koirala, D. *et al.* A single-molecule platform for investigation of interactions between G-quadruplexes and small-molecule ligands. *Nature Chem.* **3,** 782–787 (2011).

Acknowledgements

We thank T. Pope for his kind help with the phage display, W. Reik, R. Rodriguez and D. Sanders for stimulating discussions and Cancer Research UK for funding.

Author contributions

G.B. carried out the experiments, J.M. advised on the phage display and G.B., D.T. and S.B. designed the experiments. G.B., D.T. and S.B. co-wrote the manuscript.

Additional information

Supplementary information is available in the online version of the paper. Reprints and permission information is available online at http://www.nature.com/reprints. Correspondence and requests for materials should be addressed to S.B.

Competing financial interests

The authors declare no competing financial interests.

© 2013 Macmillan Publishers Limited. All rights reserved.